A ROBUST INTEGRATION BETWEEN GEOCHEMISTRY AND ADVANCED DIGITAL CORE ANALYSIS METHODS TO GENERATE HIGH-RESOLUTION POROSITY-PERMEABILITY LOGS: A CASE STUDY ON A MAJOR UNCONVENTIONAL PLAY IN MIDDLE EAST

Adnan Al-Shamali, P.K.Mishra, Naveen K. Verma and Riyad Quttainah [1],
Osama Al Jallad, Avrami Grader, Joel Walls, Safouh Kornfol and Anyela Morcote [2].
[1] Kuwait Oil Company, [2] Ingrain Inc.

This paper was prepared for presentation at the International Symposium of the Society of Core Analysts held in Vienna, Austria, 27 August – 1 September 2017

ABSTRACT

In Kuwait, the unconventional source and reservoir rock represented by Najmah Formation is characterized by a complex diagenetic history and depositional variability. This complexity makes the conventional evaluation methods alone insufficient to determine porosity and permeability logs accurately. A major goal of this study was to produce high-resolution porosity-permeability logs for Najmah Formation using advanced digital analysis and geochemistry measurements.

Sixty (60) feet of continuous core were analyzed from an oil field in South West Kuwait. The analysis started with dual-energy x-ray CT scanning of full-diameter whole core and core gamma logging. Plug litho-samples were selected to represent the varying porosity and organic matter content along the entire core length. Two-dimensional Scanning Electron Microscopy (2D SEM) and three-dimensional Focused Ion Beam (3D FIB-SEM) images were acquired and analyzed to accurately determine the kerogen content and porosity. Matrix permeability was directly computed from the 3D FIB-SEM images using the Lattice Boltzmann method. The SEM porosity was calibrated by determining the amount of movable hydrocarbons at in-situ reservoir conditions based on geochemical analyses (XRF, XRD and LECO), pyrolysis indices, Pressure-Volume-Temperature (PVT) data and desorption and adsorption isotherm experiments.

The digitally obtained porosity and permeability data showed a unique trend that was used to produce permeability at the core level. The integration between digital analysis and geochemistry data increased the estimated porosity and confirmed higher mobile hydrocarbon in the reservoir in comparison with the measured data at the surface. This produced a new porosity-permeability trend that was more representative of the reservoir conditions and caused a significant increase in the rock permeability.

The integration between the digital SEM analysis and the geochemical measurements was key in estimating in-situ porosity and permeability characteristics of the tight formation

under study. Moreover, this analysis provided an important tool for obtaining different high-resolution porosity and permeability logs based on various porosity considerations (effective, organic, inorganic, clay). This would lead to increase certainty of reservoir properties by quantifying sensitivities of TOC, porosity, and permeability and their impact on volume of mobile hydrocarbons thus increasing the net pay in the main reservoir interval.

INTRODUCTION

The Najmah Formation (Callovian-Oxfordian) was deposited in Gotnia intra-shelf basin which developed within the Arabian Plate during Mid-Jurassic and Late Mid-Jurassic period [3], [12], [9]. It is mainly composed of tight, organic matter rich argillaceous and bituminous lime mudstone interbedded with oncoidal and bioclastic packstone [3], [12], [10]. Petrophysically, it is characterized by average matrix porosity ranging from 2 to 6% and low permeability ranging from 0.01 to 1.5 mD, thus it is considered as unconventional play [9].

Its Mid-unit was deposited under anoxic/euxinic outer ramp conditions which lead to preserving large quantities of kerogen type II within its matrix. Consequently, it became one of the best hydrocarbon source rock in Jurassic section in Kuwait and the Middle East [3], [9]. Besides to its important role as a source rock, it is also acting as a reservoir and seal rocks with significant light oil production from fractured carbonate limestone intervals in Kuwait [3], [9].

Najmah Formation is also highly heterogeneous laterally and vertically due to the variability of its depositional environments (inner ramp to starved basin) and diagenetic alteration [12], [10]. Further, literature emphasized that heterogeneity of the shale rocks is observable at multiple scales starting from core up to nano-scales. Such heterogeneity was found to be the main controlling factor on the type of pores, texture of the rock and porosity versus permeability relations within the Middle East shale rocks [2], [7]. Accordingly, the conventional methods alone will not be sufficient to characterize shales and identify their sweet spots.

Additionally, within the oil window, part of this preserved organic carbon will be converted into movable crude oil and non-movable bitumen under subsurface conditions [4]. However, in standard logging analysis methods, the non-moveable oil and remaining kerogen are calculated as potential moveable oil [4]. Consequently, the derived logging data (e.g. porosity and permeability logs) from mature source rocks will be overestimated and successively will affect the estimated original oil in place (OOIP) and yield unreliable field development and production plans. This has been recognized in the open-hole porosity log recorded in Najmah source rock under investigation.

Therefore, this study aims at presenting a solution to accurately characterize the source rocks of Lower Mid- and Lower Najmah Formation through an advanced integrative workflow combining digital analysis and geochemistry measurements to generate high resolution porosity-permeability logs. These logs can support estimating an accurate (OOIP) and yield reliable field development and production plans.

METHODOLOGY

Sixty (60) feet of continuous whole cores were imaged at a resolution of 0.5 mm/voxel by Dual Energy (DE) X-ray CT scanning technique [15], [1], [7] to produce high resolution effective atomic number (Zeff) and bulk density (Rhob) logs with data point every 0.5 mm. Later, the whole cores underwent core gamma measurements. These produced logs were used to select plug samples representing the varying porosity and organic matter content along the entire core length. Afterward, detailed geochemical lab analyses represented by XRD, EDS, XRF and pyrolysis were used to determine the extracted core plugs mineralogical composition, total organic carbon (TOC) content, kerogen types and its degree of maturation. Also, Mercury Injection Capillary Pressure (MICP) analysis was performed on all extracted samples to obtain the size distribution of pore throats (PTSD). This will help in determining the optimum resolution needed to resolve the pore systems hosted within the shale samples.

Successively, two-dimensional Scanning Electron Microscopy (2D SEM) and three-dimensional Focused Ion Beam (3D FIB-SEM) images were acquired at resolutions ranging from (10 to 5 nm/voxel). Both 2D and 3D SEM images were segmented digitally by separating pore spaces from inorganic matrix grains and organic matters to determine their kerogen content and porosity at pore level. Also, the segmented 3D FIB-SEM images were used to compute the absolute permeability using the Lattice Boltzmann method [14], [6].

Finally, the quantified SEM porosities and permeabilities were calibrated digitally by removing the amount of movable hydrocarbons at in-situ reservoir conditions based on geochemical data, PVT data and adsorption isotherm experiments. This lead to generate a calibrated porosity versus permeability trend which helped in upscaling the porosity and permeability at the core level and hence generating high-resolution porosity and permeability logs.

RESULTS AND DISCUSSION

DE and Spectral Core Gamma

DE and Core Gamma data provide early visibility into the critical properties of the whole core through continuous high-resolution rock property logs. These logs help in determining the organic matter rich sweet spots for the sample selection. Also, the acquired gray and color-scale images give quick insight on the sedimentary structure and fabric of the rocks as well as their porosity types.

DE gray-scale images illustrate that these cores are highly heterogeneous with alternating layers of laminated and massive limestones (Figure1). The laminated layers are more dominant in the top portion of the cores and have more porosity compared to the massive layer which is more dominant in the bottom portion of the cores.

Zeff (reflects mineralogy) and Rhob (reflects porosity) logs (Figure 1) confirm these observations and they reflect the abundancy of porosity as well as dolomite ($Zeff_{Dol}$=13.8) and clay minerals in the top portion of the core. On the other hand, they showed that the bottom portion of the core is more calcitic ($Zeff_{cal}$=15.7) and has less porosity. The core-

measured total GR from spectral gamma scanning is the black curve labeled SGR (Figure 4). It shows that the top part of the core is highly radioactive (average about 300 API), which is due to the existence and richness of organic matter and clay minerals [13], [5]. However, the bottom part is less radioactive (average about 100 API) which indicates lower organic matter and clay mineral contents. The brown curve labeled GRwoU is the gamma without uranium and is used to estimate clay content. The red dashed curves are from well log data and generally agree with core data, although they do not show the fine scale layers. One exception is that the well log PEFZ curve is shifted far to the right (higher values) probably because of barite mud effects on the logging tool response. By integrating both of spectral gamma and DE logs, 28 plugs were selected to represent the variations in mineralogy and porosity to characterize them geochemically and petrophysically.

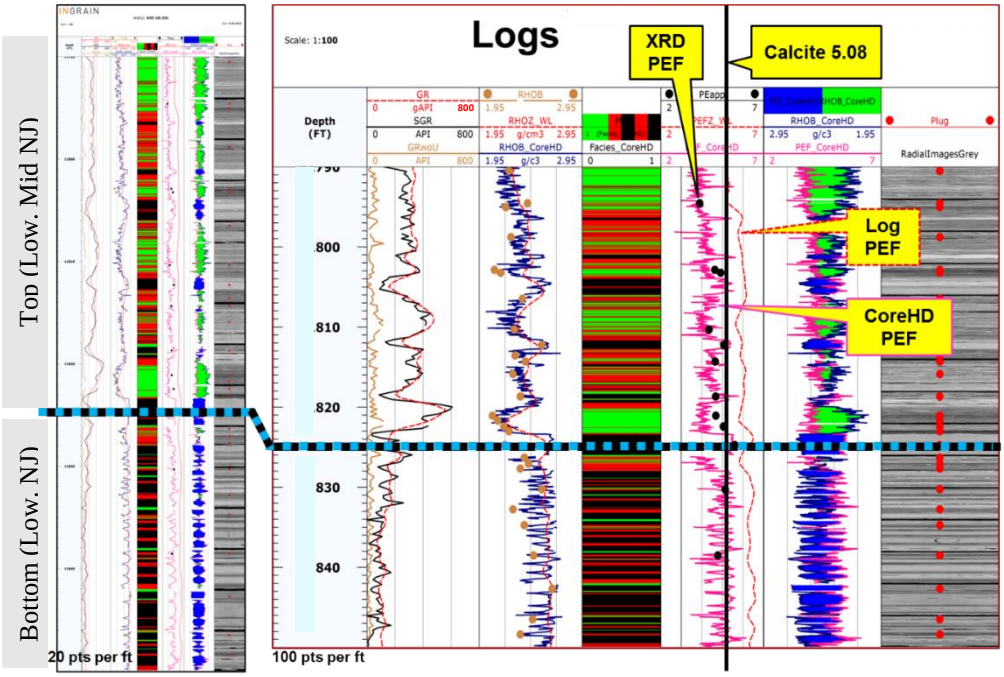

Figure 1: Spectral Gamma, Zeff and Rhob logs obtained from gamma logging and DE XCT scanning, respectively. The logs show a variation in organic matter content, mineralogical composition and porosity distribution in Najmah cores from top to bottom.

Geochemical analysis

All extracted plugs were analyzed geochemically for the purpose of quantifying their mineralogical composition and organic matter maturation and types. XRD results showed that calcite minerals are the most abundant minerals (64% in these rocks) which agrees with DE Zeff log data. The most dominant clay minerals in Najmah rock is illite with an average of 15 wt%, mainly concentrated in top portion of Najmah Formation. The organic matter within these rock samples was also characterized using LECO-TOC and Rock-Eval tests. Both tests showed that the top portion of Najmah has a high TOC content almost equal to 9 wt.% while the bottom portion has less TOC content almost equal to 5 wt.% on average which is in line with the spectral core gamma and DE logs. Additionally, the

pyrolysis analysis showed that the rock has a significant amount of crude oil "S_1" (7 mg HC/g rock in average) and non-moveable oil and solid kerogen "S_2" equal to 26 mg HC/g rock in average which indicates that this source rock has very good quality [11]. Also, they showed that the kerogen has Type II with 439ºC in average Tmax which indicates marine depositional environment and mature kerogen [11]. The Hydrogen Index (HI) is averaging at 337 which indicate mature kerogen that transformed to oil [11]. The Vitrine Reflectance "Ro" is ranging between 0.6 and 0.8 which indicates predominance of crude oil in the rock, early maturity of kerogen and existence of the rock in the oil zone [11].

Digital Rock Analysis

With assistance from the MICP derived PTSD (Figure7), the pore systems of these rocks were resolved at resolution 5 to 15 nm using 2D-SEM and 3D FIB-SEM microscopy (Figure2).

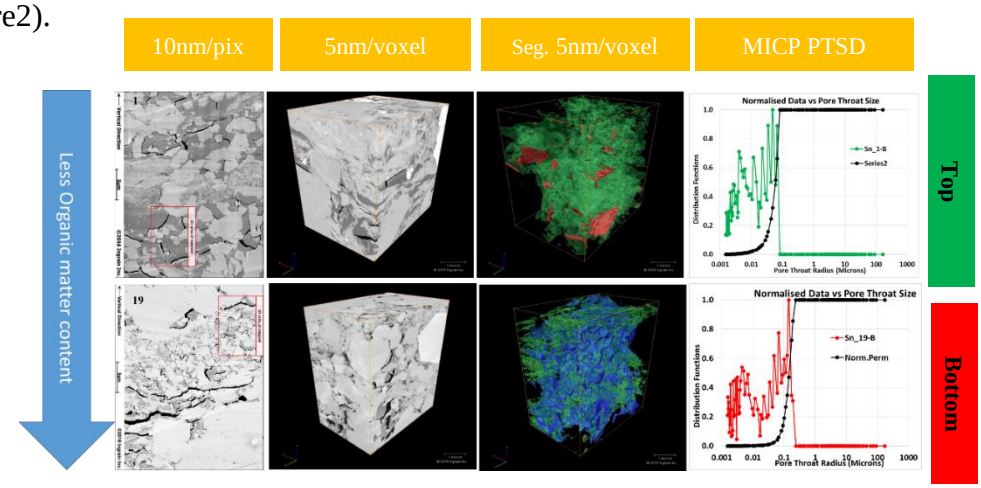

Figure 2: An example of a 3D volume and MICP analysis for SampleS #1 and 19. Green: represents organic matter. Blue: represents connected porosity, Red: represents disconnected porosity in this specific volume.

2D SEM and 3D FIB-SEM images and segmentation results showed that most of the porosity in these samples are hosted within the organic matter with average porosity equal to 5 vol. % (Figure 3b). Most of these organic pores appear to be fracture type which is dominant in the shale source rock located within oil window as illustrated in Figure (7) (Driskill et al., 2013). SEM derived TOC is in line with the measured LECO derived TOC (Figure 3a). Also, the TOC derived from SEM images showed higher average organic matter "OM" content in the top portion of Najmah core (Avg.= 22 vol.%) than its bottom portion (Avg.= 13 vol.%). This coming in line with the gamma logs, LECO test and Rock-Eval analysis.

On the other hand, the computed absolute permeabilities on Najmah samples showed a relatively high connectivity values ranging from 41 to 20017 nD. By plotting the 3D porosity versus the computed permeability, a distinct trend was obtained (Figure 3c).

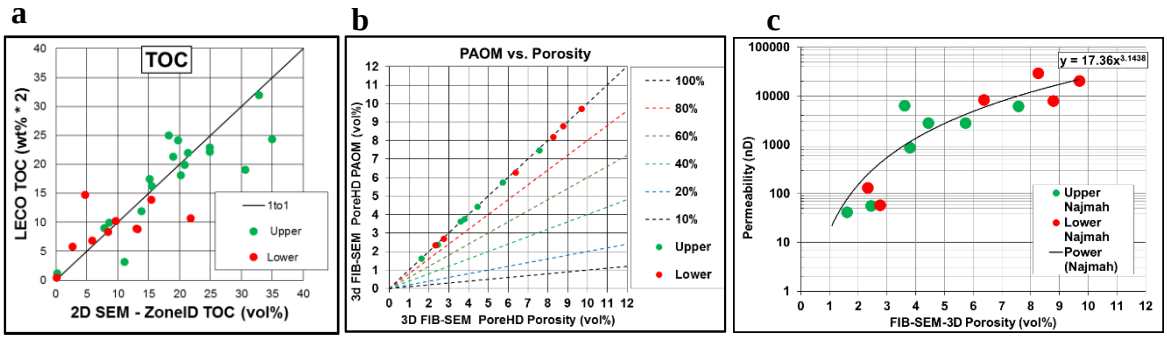

Figure 3: a) a cross plot shows the relation between the TOC quantified from SEM images and LECO TOC test. b) cross-plot shows that the majority of porosity in Najmah shale is hosted within organic matters. c) a cross-plot shows the relation between computed porosity and permeabilities in Najmah Formation

Poroperm Upscaling to Core-Scale

Porosity Correction

The main objective of this study is to generate high-resolution porosity and permeability logs for Najmah source rock using the porosity-permeability trend obtained from SEM analysis, DE derived porosity log and geochemistry data. However, the porosity defined by the 2D SEM and the 3D FIB-SEM represents the detectable effective porosity. It does not include the porosity in the clays which must be added to the effective porosity in order to be compared with the open-hole logs. A method for estimating clay-bound water (CBW) porosity has been presented by Walls, et al 2016 [16]. This method uses published data for the porosity of four pure clay minerals including illite. The apparent clay porosity for pure illite is 0.09. If we assume that essentially all of the clay in Najmah is illite (which is supported by XRD and XRF data), then the clay associated porosity is 0.15 times 0.09 or 0.014 (fractional volume). Hence, 1.4% additional porosity was added to the quantified SEM effective porosities to correct them. Additionally, the pyrolysis analysis showed that Najmah source rock is existing within the oil window in which significant volumes of kerogen has transformed to producible light "S_1" and non-producible heavy oil "x fraction of S_2". Also, the Langmuir adsorption experiment conducted on Najmah cores by Kuwait Oil Company (KOC) showed that methane was dissolved in the oil which covers the organic matter rather than adsorbed on the organic matter surfaces. Thus, the volume of porosities occupied by S_1 and x fraction of S_2 should be added to the effective porosity besides to clay porosity. Accordingly, both of Langmuir adsorption experiment, Gas Oil Ratio (GOR) and oil density derived from PVT test, and pyrolysis indices (S_1 and S_2) were integrated to calculate the amount of gas in solution – mimicking the Langmuir isotherm experiments (Figure 4). The calculations showed that if (S_1+0.4*S_2) are used (at each plug location that LECO-SRA was measured in the laboratory) a reasonable correlation between dissolved gas and the Langmuir results is obtained (Figure 4). Consequently, the equivalent volumes of S_1 and 0.4*S_2 were considered as an actual part of porosity besides to 1.4% porosity hosted within the clay minerals.

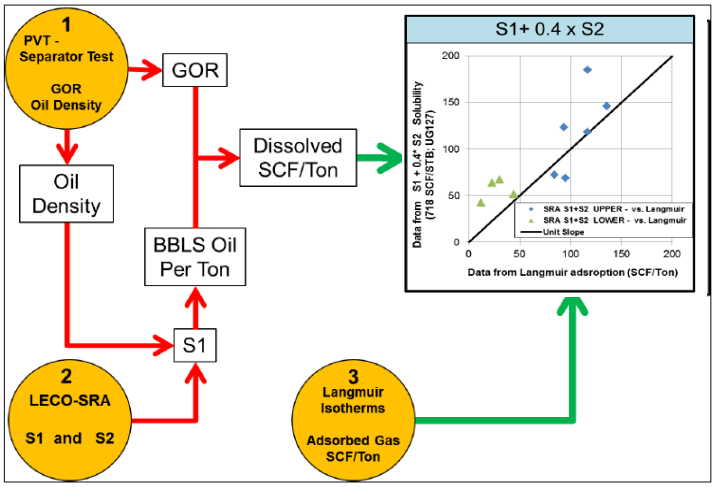

Figure 4: Workflow for computing solution gas content in SCF/Ton and the corresponding comparison between gas solubility data and Langmuir adsorption data (S_1+0.4*S_2).

After adding these porosities to the effective porosities derived from SEM (5% on average), the porosities of the samples derived from upper Najmah as well as DE derived porosity log have approximately doubled, reaching 10% on average (Figure 5). Even though the porosity of top Najmah has increased, it's still lower than the open-hole log density-porosity (25% in average). Such relatively high value of porosity wasn't observed in MICP, He and DE derived porosity measurements which are averaging 5%, similar to SEM derived porosities. This phenomenon is attributed to calculating the non-moveable oil and remaining kerogen in standard logging analysis methods as potential moveable oil [4]. By applying the corrections described above, the resultant porosity log matched reasonably well with the wireline density-porosity. The lower Najmah porosities have also increased slightly reaching to 7.5% on average which is close to the open-hole log. This is expected because of the low concentration of organic matter and crude oil towards the bottom of the Najmah Formation which resulted in more reliable logging data.

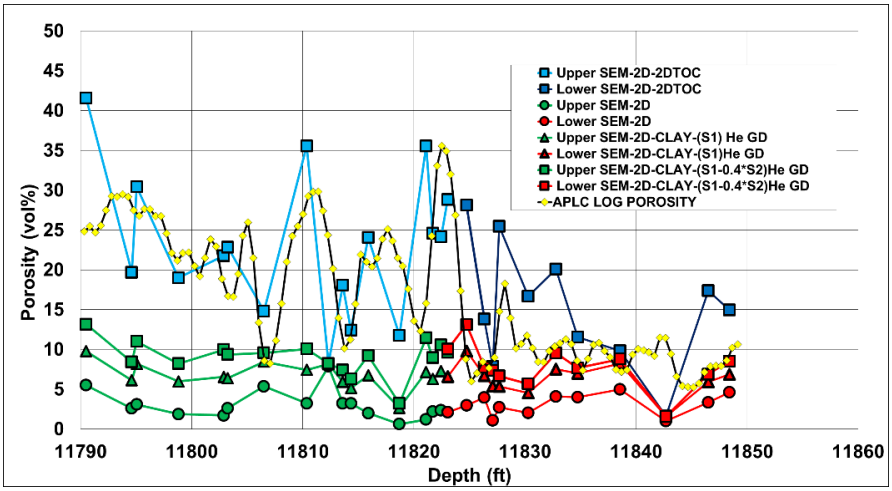

Figure 5: Estimates of total porosity which includes effective porosity, clay porosity, S1, and part of S2. Red and green circles: Effective porosity. Red and green squares: Total porosity (Effective porosity + clay porosity + S1 + 0.4*S2). The black curve with yellow dots represents the computed wireline density-porosity log. The blue curve with squares represents the plug sample total porosity plus organic material.

Porosity-Permeability Correlation Correction and Upscaling

Since effective SEM porosities of the 28 samples increased two times after applying (S1+0.4*S2+CBW) correction, the absolute permeability increased as well. Therefore, the initial 3D porosity-permeability trend obtained through DRA required correction also. Consequently, the same volume of producible TOC (residual oil (S1) + 0.4*S2) added previously was eroded digitally from the solid organic content of each 3D FIB-SEM volume and the permeability was recomputed using Lattice Boltzmann (LBM) method. The resulting new porosity-permeability trend was generated (Figure 6a), and together with the corrected DE derived porosity log, was used to generate a high-resolution permeability log at core scale (Figure 6b). The generated permeability logs showed that permeability increased by a factor of 5X to 20X. This new computed porosity-permeability trend should better represent in-situ conditions, where a significant fraction of the organic matter imaged at the surface is likely mobile and producible at reservoir temperature and pressure.

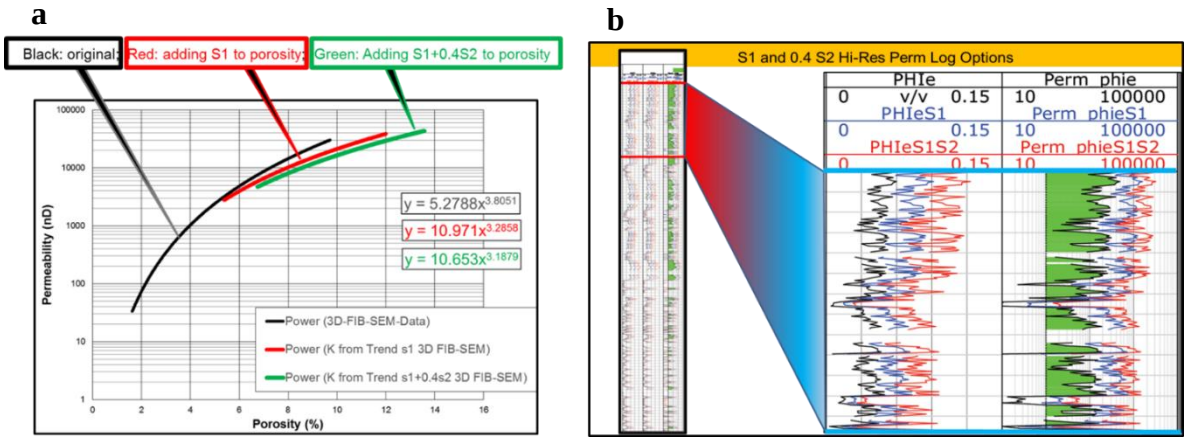

Figure 6: a) Green curve: Porosity-permeability correlation generated by eroding the producible organic matter from 3D FIB volume of each sample individually. b) High resolution porosity and permeability logs calculated after removing the S1+0.4*S2+Clay porosity from effective porosity.

SUMMARY and CONCLUSIONS

1- The integration between the digital SEM analysis and the geochemical measurements was key in estimating in-situ porosity and permeability characteristics of the tight formation under study.
2- This link provides the constraints for adjusting the distribution and balance of organic porosity and organic matter and yields different poro-perm scenarios and improved reservoir characterization which leads to:
    a. Higher accuracy in determining reservoir properties for improved quantification of reserves and productivity.
    b. Increase certainty of reservoir properties by quantifying sensitivities of TOC, porosity, and permeability and their impact on volume of mobile hydrocarbons thus increasing the net pay in the main reservoir interval.

ACKNOWLEDGEMENTS

Ingrain Inc. would like to thank KOC NFD-l (WK) and R&T- Subsurface Teams for their contributions and support through the course of this study. The keen interest shown by Dr. Prasanta Kkumar Mishra, Senior Geologist, Adnan Aiesh Al-Shamali, Team Leader and Mr. Naveen Verma, Tpl Specialist I (geology) is gratefully acknowledged.

REFERENCES

1. *Al-Owihan, H., Al-Wadi, M., Thakur, S., Behbehani, S., Al-Jabari, N., Dernaika, M., & Koronfol, S. (2014). Advanced Rock Characterization by Dual Energy CT Imaging: A Novel Method in Complex Reservoir Evaluation. International Petroleum Technology Conference. doi:10.2523/iptc-17625-ms*
2. *Almarzooq, A., Alghamdi, T., Koronfol, S., Dernaika, M., & Walls, J. (2014). Shale Gas Characterization and Property Determination by Digital Rock Physics. SPE Saudi Arabia Section Technical Symposium and Exhibition. doi:10.2118/172840-ms.*
3. *Alsharhan, A. S., & Nairn, A. E. (2003). Sedimentary basins and petroleum geology of the Middle East. Amsterdam: Elsevier.*
4. *Asquith, G. B. (2015). OOIP Utilizing GEOCHEM [ECS] Data, Triple Combo Data Only, and Pyrolysis S1 Data, Permian Wolfcamp "A" and "B" Shales, Midland Basin, Texas. AAPG Search and Discovery , article# 110207.*
5. *Bigelow, E. L. (1992). Introduction to Wireline log analysis. Houston: Western Atlas International.*
6. *De Prisco, G., Toelke, J., & Dernaika, M. (2012). Computation of relative permeability functions in 3D digital rocks by a fractional flow approach using the lattice Boltzmann method. SCA, 36. Aberdeen, Scotland.*
7. *Dernaika, M., Jallad, O. A., Koronfol, S., Suhrer, M., Walls, J., & Matar, S. (2015). Petrophyscial and Fluid Flow Properties of a Tight Carbonate Source Rock Using Digital Rock Physics. Proceedings of the 3rd Unconventional Resources Technology Conference. doi:10.15530/urtec-2015-2154815.*
8. *Driskill, B., Walls, J., Sinclair, S. W., & DeVito, J. (2013). Applications of SEM Imaging to Reservoir Characterization in the Eagle Ford Shale, South Texas, USA. AAPG Memoir , 102, 115-136.*
9. *Khan, B., Nohut, O., Steene, M. V., Ghneej, A. A., & Ajmi, A. A. (2014). Petrophysical Evaluation of Unconventional Najmah Formation of Kuwait - A Case Study. Proceedings 76th EAGE Conference and Exhibition 2014. doi:10.3997/2214-4609.20141390.*
10. *Khan, D., & Al-Ajmi, M. (2016). Depositional architecture of the Gotnia basin during Oxfordian in southern part of Kuwait. International Conference and Exhibition, Barcelona, Spain, 3-6 April 2016. doi:10.1190/ice2016-6459957.1*
11. *McCarthy, K., Rojas, K., Niemann, M., Palmowski, D., Peters, K., & Stankiewicz, A. (2011). Basic Petroleum Geochemistry for Source Rock Evaluation. Schlumberger Oil Review , 23(2), 32-43.*

12. *Ray, D. S., Al-Shammeli, A., Al-Khamees, W., Fuchs, M., & Groen, V. D. (2013). Depositional and Diagenetic Sedimentological Model of Najmah-Sargelu Formation, Umm Gudair, Kuwait. International Petroleum Technology Conference. doi:10.2523/iptc-17117-ms.*
13. *Russell, W. L. (1944). The Total Gamma Ray Activity Of Sedimentary Rocks As Indicated By Geiger Counter Determinations. Geophysics, 9(2), 180-216. doi:10.1190/1.1445076.*
14. *Tölke, J., Prisco, G. D., & Mu, Y. (2013). A lattice Boltzmann method for immiscible two-phase Stokes flow with a local collision operator. Computers & Mathematics with Applications, 65(6), 864-881. doi:10.1016/j.camwa.2012.05.018.*
15. *Walls, J., & Armbruster, M. (2012). Shale Reservoir Evaluation Improved by Dual Energy X-Ray CT Imaging. Journal of Petroleum Technology, 64(11), 28-32. doi:10.2118/1112-0028-jpt*
16. *Walls, J., D. Buller, A. Morcote, M.L. Everts, B. Guzman, Integration of Whole Core, Drill Cuttings, and Well Log Data for Improved Characterization in the Wolfcamp Formation, Unconventional Resources Technology Conference (URTeC) DOI 10.15530-urtec-2016-2461526*